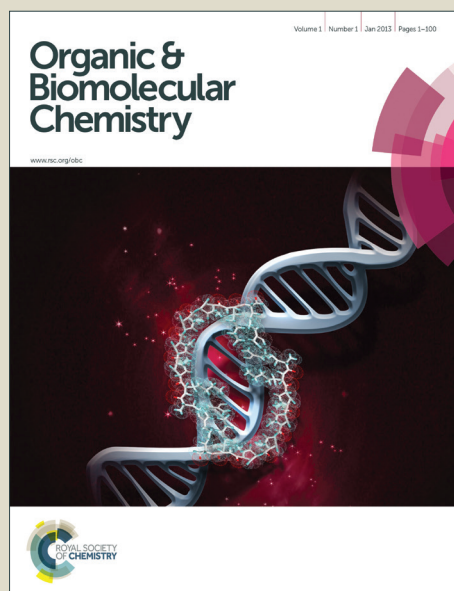


# Organic & Biomolecular Chemistry

Accepted Manuscript



This is an *Accepted Manuscript*, which has been through the Royal Society of Chemistry peer review process and has been accepted for publication.

*Accepted Manuscripts* are published online shortly after acceptance, before technical editing, formatting and proof reading. Using this free service, authors can make their results available to the community, in citable form, before we publish the edited article. We will replace this *Accepted Manuscript* with the edited and formatted *Advance Article* as soon as it is available.

You can find more information about *Accepted Manuscripts* in the [Information for Authors](#).

Please note that technical editing may introduce minor changes to the text and/or graphics, which may alter content. The journal's standard [Terms & Conditions](#) and the [Ethical guidelines](#) still apply. In no event shall the Royal Society of Chemistry be held responsible for any errors or omissions in this *Accepted Manuscript* or any consequences arising from the use of any information it contains.

# Quantum Mechanistic insights on Aryl Propargyl Ether Claisen Rearrangement

Venkatesan Srinivasadesikan<sup>‡</sup>, Jiun-Kuang Dai<sup>†</sup> and Shyi-Long Lee<sup>†\*</sup>

<sup>†</sup>*Department of Chemistry and Biochemistry, National Chung Cheng University, Taiwan*

<sup>‡</sup>*Department of Applied Chemistry, National Chiao Tung University, Hsinchu, Taiwan.*

## Abstract:

The mechanism of aryl propargyl ether Claisen rearrangement in gas and solvent phase has been investigated using DFT methods. The solvent phase calculations are carried out using N, N-diethylaniline as a solvent in PCM model. The most favorable pathways involves [3,3]-sigmatropic reaction followed by proton transfer in the first two steps and then deprotonation or [1,5]-sigmatropic reaction. Finally, the cyclization yields benzopyran or benzofuran derivatives. The [3,3]- sigmatropic reaction is the rate-determining step for benzopyran and benzofuran with  $\Delta G^\ddagger$  value of 38.4 kcal/mol and 37.9 kcal/mol at M06/6-31+G\*\*//B3LYP/6-31+G\* level in gas and solvent phase, respectively. The computed results are in good agreement with the experimental results. Moreover, it is found that the derivatives of aryl propargyl ether proceeded Claisen rearrangement and the rate-determining step may be shifted from the [3,3]-sigmatropic reaction to the tautomerization step. The NBO analysis is revealed that the substitution of methyl groups on aliphatic segment has decreased the stabilization energy E (2) and favors the aryl propargyl ether Claisen rearrangement.

Corresponding Author: chesll@ccu.edu.tw

## Introduction

The Claisen rearrangement is a versatile tool in organic synthesis to form carbon-carbon bond<sup>1</sup> and the first recorded example of [3,3]-sigmatropic reaction<sup>2</sup>. Since it was discovered in 1912, this reaction has continued to be advanced in the methods or in the applications towards the total synthesis of natural products and pharmacologically relevant molecules. The benzofuran and benzopyran derivatives are ubiquitous in nature and also serve as versatile synthetic intermediates in pharmaceuticals. Those compounds can be obtained easily by aryl propargyl ether Claisen rearrangement<sup>3</sup> and the mechanism has been speculated by Zsindely and Schmidt<sup>4</sup>. However, there are few experimental reports on the aryl propargyl ether Claisen rearrangement has been reported<sup>3,4,5-10</sup> and there is a need of Quantum mechanical calculation to support the mechanistic speculation. In this paper, detailed Quantum mechanical calculations have been carried out for all the plausible mechanisms and presented.

There are a number of approaches for the synthesis of benzofuran and/or benzopyran<sup>11-24</sup>. However, most of the methods suffer from one or more disadvantages including low yield, toxic and expensive reagents, long reaction time and environmental pollutions and so on. In addition, some of these approaches are a lack of flexibility in terms of substituents. Otherwise, a simple route was reported by Iwai and Ide which was established for the rearrangement of simple aryl propargyl ether in N, N-diethylaniline at higher temperature yielded the benzopyrans<sup>3</sup> but the yield was not ideal. Moreover, the substituent effect of aryl propargyl ether was also discussed to increase the yield<sup>5-9</sup>. After a number of detailed examination of aryl propargyl ether Claisen rearrangement, a route in presence of cesium fluoride (CsF) leading to formation of 2-methylbenzofuran in excellent yield was reported by Ishii *et*

*al.*<sup>10</sup>. Therefore, the thermal rearrangement of aryl propargyl ether leads to an effective and convenient procedure for yielding the benzopyran or benzofuran. Lingam *et al.* also explained that the rearrangement has highly functionalized property<sup>19</sup>. However, when the meta-substituent aryl propargyl ether proceeded *via* the Claisen rearrangement, it has been observed with two orientations can be carried out to yield two different products that we denoted as ortho- and para-cyclized product with regioselectivity. Anderson *et al.* have been attempted to provide the reasonable explanations for the regioselectivity<sup>8-9</sup>. Unfortunately, this is difficult without knowing which step is the rate-determining step that affects the substituent effects and then influences the final yield. Therefore, it is important to realize the complete mechanism of aryl propargyl ether Claisen rearrangement.

Since 1984 the Claisen rearrangement has been studied theoretically,<sup>25</sup> which used MNDO to analyze the transition state structures. Since then, a number of Claisen rearrangements have been reported by semi-empirical, *ab initio* and DFT computational studies. But, most of the studies concentrated on allyl vinyl ethers and aryl vinyl ethers. The computational reports on Claisen rearrangement were such as Ireland-Claisen rearrangement for the effects of substituents on the transition state and for the stereoselectivity<sup>26-27</sup>, Gosteli-Claisen rearrangement for describing the substituent rate effect quantitatively<sup>28</sup> and “on water” reaction to know the reactivity for the aromatic Claisen rearrangement by QM/MM methods<sup>29-30</sup>. However, there is a lack of theoretical aryl propargyl ether Claisen rearrangement and the reaction is an important for the synthesis of benzopyran or benzofuran. Moreover, the rate-determine step is also uncertain. Therefore, in the present work we set out to obtain the plausible mechanistic pathways and also to recognize the rate-determining step by the state-of-the-art quantum mechanical methods.

In this article, the reaction pathways in scheme 1 are examined and then the

rate-determining step is determined from the Potential Energy Surface (PES) by DFT calculations. Moreover, the rate constant of the reactions has also been calculated to examine which method is suitable to describe the systems. The rationalized discussion has also been presented for the product of benzopyran and benzofuran from aryl propargyl ether using the potential energy surface. Subsequently, the substituent effects, NBO analysis and pKa results have been discussed.

## Computational Methods

### 1. Computational Methods

Geometry optimizations have been performed at B3LYP<sup>31-35</sup> with the basis set 6-31+G\*. The same level of method was used for the frequency calculations at all the optimized structures. Zero Point Vibrational Energy (ZPVE) corrections are included in the total energy. The Intrinsic Reaction Coordinate (IRC) calculations have also been carried out to verify the identity of the Transition State (TS) structures and to obtain the potential energy surface profile connecting the TS to the two associated minima of the proposed mechanisms. Single-point energy calculation is performed by different DFT methods (M06-2X<sup>36</sup>, M05-2X<sup>37</sup>, M06<sup>36</sup>, M05<sup>38</sup>,  $\omega$ B97XD<sup>39</sup>, BMK<sup>40</sup>, B2PLYP<sup>41</sup>) with the basis set of 6-31+G\*\*. The solvation energies are computed using N, N-diethylaniline ( $\epsilon = 5.5$ ) as a solvent with Self-Consistent Reaction Field (SCRF) method using Polarized Continuum Model (PCM)<sup>42-43</sup>. All calculations have been performed with the Gaussian 09 package<sup>44</sup>.

Natural bond orbital (NBO)<sup>45-46</sup> analysis are performed at M06/6-31+G\*\*//B3LYP/6-31+G\* level using NBO 3.0 version included in Gaussian 09 package. All possible interactions between filled (donor) Lewis type and empty (acceptor) non-Lewis type NBOs, and estimating their energies by 2<sup>nd</sup>-order perturbation theory. For each donor NBO (i) and acceptor NBO (j), the stabilization

energy  $E(2)$  associated with delocalization  $i \rightarrow j$  is estimated as

$$E(2) = \Delta E_{ij} = q_i \frac{(F(i, j))^2}{\varepsilon_j - \varepsilon_i}$$

where  $q_i$  is the donor orbital occupancy,  $\varepsilon_j$ ,  $\varepsilon_i$  are diagonal elements (orbital energies) and  $F(i, j)$  is the off-diagonal NBO Fock matrix element. The larger  $E(2)$  value indicates that the interaction between donor and acceptor is stronger.

## 2. Comparison for Different DFT Methods

A benchmark study has been carried out for aryl propargyl ether Claisen rearrangement in order to evaluate the DFT methods on the activation energy. Our computed activation energies can be compared with the experimental rate constants<sup>7</sup>. Recently, Ramadhar *et al.* has also reported a benchmark study to evaluate the performance of different DFT methods on the activation barrier ( $\Delta G^\ddagger$ ) for the aliphatic-Claisen rearrangement and indicated that single point energies computed by M05, M06 and M08 functionals on B3LYP optimized structures could give better estimated values<sup>47</sup>. The optimization as well as frequency analysis are carried out at B3LYP/6-31+G\* level, then the single-point energies are computed by different DFT methods (B3LYP, M06-2X, M06, M05-2X, M05, wB97XD, BMK and B2PLYP) with the basis set of 6-31+G\*\* in the solvent -phase. The calculated results are shown in Table 2.

As seen in Table 2, M06 and M05 methods provide better results with the Root Mean Square Error (RMSE) of 1.4 kcal/mol and 1.2 kcal/mol, respectively, and Mean Unsigned Error (MUE) of 1.0 kcal/mol and 1.1 kcal/mol, respectively. The M06 functional is selected to further examine the basis set effects. The results of M06 with different basis set size are shown in Table 3. As seen in Table 3, while increasing the basis set size the RMSE and MUE values are decreasing slightly and levels out at 6-31+G\*\* for M06 functional. It suggests that a more flexible basis set than 6-31+G\*\* may not be beneficial to prediction of the energy barriers for aryl propargyl ether Claisen rearrangement. Based on the aforementioned analysis, the M06/6-31+G\*\*//B3LYP/6-31+G\* level has the best performance for the eleven aryl

propargyl ether Claisen rearrangement reaction barriers with a precision of 1.3 kcal/mol and 0.9 kcal/mol for RMSE and MUE, respectively. Therefore, the M06/6-31+G\*\*//B3LYP/6-31+G\* level is adopted in our further analysis for aryl propargyl ether Claisen rearrangement.

## Results and Discussions

### 1. Mechanism and Structures

The plausible mechanism of aryl propargyl ether Claisen rearrangement is described in Scheme 1 and the selected geometries in gas phase are shown in Figure 1. As shown in Scheme 1, the step 1 belongs to Claisen rearrangement with a cyclic transition state (TS 1 in Figure 1). This is a reaction with a  $\sigma$  bond which migrates from one end of a  $\pi$  system to the other, that is, the breaking of C3-O4 bond and forming C1-C10 bond. In proton transfer step (Step 2), there are two possible pathways: intramolecular or intermolecular proton transfer as proposed in the previous literature<sup>30,48</sup>. The calculated results of Yamabe *et al.* indicate that the intermolecular proton transfer has more reliable mechanism than the intramolecular proton transfer in the second step of the aromatic Claisen rearrangement.<sup>48</sup> Our results also favor the intermolecular proton transfer (TS2-2) which is in good agreement with the previous report. Three possible mechanisms are then followed from Int2: one is [1,5]-sigmatropic reaction followed by an isomerization to form the benzopyran *via* cyclization, another is H abstraction followed by a cyclization to 2-methylbenzofuran and the third one is cyclization followed by [1,3]-sigmatropic reaction to 2-methylbenzofuran.

As shown in Figure 1, in the first step, the C3-O4 bond length is elongated from 1.427 Å in reactant to 1.920 Å in TS1 and further to 3.747 Å in int1. Meanwhile, the C1-C10 bond length is shortened from 3.959 Å in reactant to 2.031 Å in TS1 and further to 1.535 Å in int1. It

indicates that the C3-O4 bond breaks and C1-C10 bond formed simultaneously. In the intramolecular proton transfer process, the distances of O4-H11 and C10-H11 are 1.386 and 1.431 Å in TS 2-1, respectively, where a four-member ring is formed. Moreover, the bond angle of O4-H11-C10 is 105.7°. In TS2-2, the proton H11 transfers from C10 to O4' of the second molecule and the proton H11' transfers from C10' of the second molecule to O4 in a stepwise manner. It is worth noting that the bond angle is 172.1° for  $\angle$ C10-H11-O4' and 160.0° for  $\angle$ C10'-H11'-O4. These bond angles are larger than the bond angles in TS 2-1 and leading to a smaller ring strain. The results show that the intermolecular proton transfer is feasible than intramolecular counterpart. In TSa3 (pathway A) the O4-H11 bond length is 1.260 Å and C2-H11 bond length is 1.335 Å. It shows that the hydrogen is shared by C2 and O4. Subsequently, the isomerization proceeds after [1,5]-sigmatropic reaction, and then the C3-O4 bond length is shortened about 1.474 Å *via* cyclization forming the benzopyran (product A). The pathway B is a dissociation reaction; in allenic phenol, Int 2, the deprotonation occurs to form the allenic phenolate Intb2. Finally, the last step is a cyclization, where O4-C2 bond length is shortened about 1.418 Å (Intb2 to product B) and forming the 2-methylbenzofuran. For the pathway C, cyclization reaction, the O4-C2 bond length is shortened by 1.378 Å (Int2 to IntC3), and it undergoes the [1,3]-sigmatropic reaction in which H11 is partially coordinated between C1 and C3 (1.725 Å and 1.956 Å, respectively) of TS4 to form the 2-methylbenzofuran. In pathway B, one of the steps has proceeded through the O-H dissociation. Thus, the pKa<sup>49</sup> is calculated to provide the ability of hydrogen abstraction. (See Table S10). The pKa results show that the Chloro- substituents at aryl group makes the proton abstraction easier and helps to proceed and facilitates the formation of 2-methyl-benzofuran.

## 2. Potential Energy Surface and Reaction Mechanism.

The relative potential energy surface for aryl propargyl ether Claisen rearrangement in



gas and N, N-diethylaniline phase is shown in Figure 2 and detailed informations are in Table 1. The plausible mechanisms for aryl propargyl ether Claisen rearrangement is known to be pericyclic. The pericyclic reaction pathway can be observed from TS1, TS2-1 and TS2-2. As shown in Table 1, it can be observed that the difference between the Gibbs free energy of gas-phase and solvent phase is larger because the Intb2, TSb3 and Product B complex have ionic species. The variations for other TS and Int in gas-phase and solvent phase are not too large (about 0.8 kcal/mol). Therefore, following discussion is based on solvent phase results. Also, the experimental reactions have been carried out using the N, N-diethylaniline as a solvent.

As seen from Fig. 2, for TS1 in solvent phase, the energy barrier of C3-O4 bond breaking and C1-C10 bond forming is 37.9 kcal/mol with the loss of aromaticity. The intramolecular (TS2-1) & intermolecular (TS2-2) proton transfer occurs with the energy barrier of 52.1 and 33.6 kcal/mol, respectively. The lowest energy barrier of intermolecular proton transfer is energetically favorable than the intramolecular proton transfer. Three different pathways have been followed from the allenic phenol intermediate (Int2). For the pathway A, the energy barrier is 25.2 kcal/mol for [1,5]-sigmatropic reaction and 11.5 kcal/mol for cyclization. Meanwhile, the isomerization requires overcoming the energy barrier of 10.7 kcal/mol. The isomerization takes place from s-trans conformation (Inta3) to s-cis conformation (Inta4) and finally yields benzopyran (Product A). The energy barrier has decreased chronologically from Int2 to Product A, in pathway A, owing to the extended conjugation cycle and finally end up with the oxa-diels-alder reaction to form the benzopyran. Overall, the reaction in pathway A has to be considered as a concerted reaction. For the pathway B, the dissociation energy ( $D_e$ ) of Intb2 is too high about 207 kcal/mol. Cyclization from allenic phenolate, Intb 2, to form the product B complex *via* TSb3 requires the energy barrier of 16.8 kcal/mol. Further, the abstraction of  $H^+$  yields the 2-methylbenzofuran, exothermic, with large formation energy. The pKa has been calculated for O-H dissociation in

allenic phenol (Int2). The pKa calculations have been performed at M06/6-31+G\*\*//B3LYP/6-31+G\* in gas and solvent phase which included both thermodynamic cycles. The pKa values have been listed in Table S10. The acidic nature of allenic phenol can be observed from the value of pKa. The acidity of allenic phenol (Int2) is quite higher compared to phenol.<sup>50</sup> The value of pKa has increased while increasing the number of methyl groups at C3 position, due to the steric hindrance near to the -OH group. The pKa cycle and results clearly suggest that the strong base is required to achieve the benzofuran product (Product B) experimentally. Also, the substitution of methyl and methoxy groups has increased the pKa value while chloro substitution has decreased the pKa along with methyl groups at C3 position due to the inductive effect. In the pathway C, allenic phenol (Int2) precedes the cyclization *via* 70.8 kcal/mol energy barrier, and follows [1,3]-sigmatropic rearrangement which requires the energy of 67.2 kcal/mol to form the 2-methylbenzofuran. The energy barrier of the pathway C is higher and it has not been discussed further.

The TS1, TS2-1 and TS2-2 may be considered as pericyclic reactions, due to their higher energy barrier than the rest of the successive pathways. Int2 onwards the mechanism has followed the three different plausible pathways to yield the benzofuran and benzopyran moieties. In pathway A, the TSa3 and TSa4 barrier energy is lower compared with the TS1 and TS2-2. In TSa3 the phenolic bond is broken with one orbital disconnection at oxygen. Also, in TSa5 the ether bond is forming through oxa-diels-alder reaction. Overall, the pericyclic reactions (TS1, TS2-2) is followed by bond breaking and bond forming reactions with the low barrier energy due to the extended conjugation in TSa3 and TSa5.

From Figure 2 and Table 1, the energy barrier of [3,3]-sigmatropic reaction is 37.9 kcal/mol for TS1. The energy barrier for the O4-C10 bond breaking and C1-C10 bond formation are key steps in aryl propargyl ether Claisen rearrangement. From the energy barrier, it can be concluded that the [3,3]-sigmatropic reaction is the rate-limiting step for the

pathway A and pathway B. In summary, the pathway A and B are more favorable for benzopyran and 2-methyl-benzofuran, respectively, in overall mechanism.

From the thermodynamic properties, the Gibbs free energies of the final products benzopyran and 2-methyl-benzofuran are -37.1 kcal/mol and -51.1 kcal/mol in solvent phase, respectively. It is worth noted that only the energy of allenic dienone, Int 1, related to the reactant is positive owing to the loss of its aromaticity. The first step is the rate-determining step and its energy barrier is 37.9 kcal/mol, and the followed barrier of reaction is lower. Moreover, the energy barrier for the TSa4 is 10.7 kcal/mol which is a simple isomerization of -trans to -cis conformation. In pathway A, the exocyclic extended conjugation plays a crucial role for the low energy barrier. Therefore, once beyond the rate-determining step and followed step has enough energy to precede the reaction quickly. The formation of 2-methyl-benzofuran is more exothermic than benzopyran formation, that is, the 2-methyl-benzofuran is more stable than the benzopyran.

### 3. Substituent Effects

In order to understand the substituent effects on the kinetics of aryl propargyl ether Claisen rearrangement, the substitutions on aryl and aliphatic segment are considered. Scheme 2 represents the possible substitution sites on aryl propargyl ether. The Methyl, Methoxy and Chloro have been considered as a substitution groups at ortho-, meta- and para-positions in aromatic ring for the study. The meta-substitution has two possible reaction orientations and gives a mixture of ortho- and para-cyclized products.

Table 4-6 presents the energy barrier for the first two steps of bond breaking and new bond forming reactions for the Methyl, Methoxy and Chloro groups on aromatic and methyl group on aliphatic segment of the reactant in solvent phase at M06/6-31+G\*\*//B3LYP/6-31+G\* level. The substitution at meta-2 position favors the ortho-cyclized product due to the lower energy barrier. Moreover, the energy barriers are

found to be decreased when the number of methyl groups at C3 position has increased for the above mentioned three different functional groups on aromatic ring. From the results, it can be concluded that the Methyl, Methoxy and Chloro groups at o,m, and p positions on the aromatic segment decreases the energy barrier slightly and the methyl groups at C3 position has reduced the energy barrier greatly. However, these substituents do not affect the tautomerization of the reaction, remarkably. Therefore, step 2, the proton transfer reaction becomes the rate-determining-step.

Besides, the C3-O4 and O4-C5 bond can rotate freely for the aryl propargyl ether and produce different conformational isomers. Fig. 3 shows the geometric structures for the two lowest energy conformational isomers. As seen in Fig. 3, when the number of methyl group increases the energy difference become larger from 0.6 kcal/mol to 2.1 kcal/mol. Therefore, the substitution of more methyl groups at C3 position is found to be a better orientation for the reactant to facilitate the aryl propargyl ether Claisen rearrangement.

NBO analysis<sup>45-46</sup> have also been performed to rationalize the aforementioned results as increasing the number of methyl groups at C3 position which facilitates the aryl propargyl ether Claisen rearrangement. NBO analysis are carried out for the transition state structures of A, B and C shown in Fig. 4. Donor-acceptor stabilization energies from NBO analysis for these three transition state structures are collected and listed in Table 7. As can be seen in Table 7, for each transition state structures, the donor-acceptor interaction involves  $\pi \rightarrow \pi^*$  and  $\pi^* \rightarrow \pi^*$  between C5-O4 and C2-C3, the  $\sigma \rightarrow \pi^*$  between C1-C10 and C5-O4, and the  $\sigma \rightarrow \pi^*$  between C1-C10 and C2-O3 contribute to their stabilization energy. The total stabilization energies are 157.08, 141.19, 126.71 kcal/mol for transition state structures of A, B and C, respectively. Larger stabilization energy results with higher energy barrier in step 1 have blocked the aryl propargyl ether Claisen rearrangement. In other words, methyl group substitution at C3 position has revealed the smaller stabilization energy and thus decreases the energy barrier which helps to facilitate the aryl propargyl ether Claisen rearrangement.

## Conclusion

Three possible pathways for aryl propargyl ether Claisen rearrangement have been investigated. The pathway A and pathway B are the most possible routes to form the benzopyran and benzofuran, respectively. The rate-limiting step is the first step in aryl propargyl ether Claisen rearrangement with  $\Delta G^\ddagger$  are 38.4 and 37.9 kcal/mol in gas and solvent phase, respectively, for parent aryl propargyl ether. Different DFT methods are performed to check the energy barrier and the results at M06/6-31+G\*\*//B3LYP/6-31+G\* level are in good agreement with the experimental values. At this level, the MUE and RMSE values are 1.0 and 1.4 kcal/mol, respectively. For the substituent effects, one can find the energy barrier for the substituent in the para-position is higher than those in ortho- and meta- positions. The substitution of methyl groups at C3 position lead to decrease the energy barrier dramatically and change the rate-limiting step from the [3,3]-sigmatropic reaction to proton transfer step. According to the results of structural information, the substitution of methyl groups at C3 position make the C3-O4 bond lengthen from 1.43 Å to 1.45 Å and C1-C10 bond shorten from 3.97 Å to 3.70 Å in the reaction center of aryl propargyl ether. In addition, the methyl groups at C3 position might lead to the correct orientation for the reaction to proceed. Also, the donor-acceptor NBO results suggest that the methyl group substitution at C3 position helps to precede the aryl propargyl ether Claisen rearrangement reaction smoothly.

## ACKNOWLEDGMENT

This research was supported by the National Science Council (NSC) of Taiwan, and the computational resource is partially supported by National Center for High-Performance Computing (NCHC), Hsin-Chu, Taiwan. We also greatly acknowledged Dr. Yu-Wei Huang for his valuable assistance and discussion at the time of work.

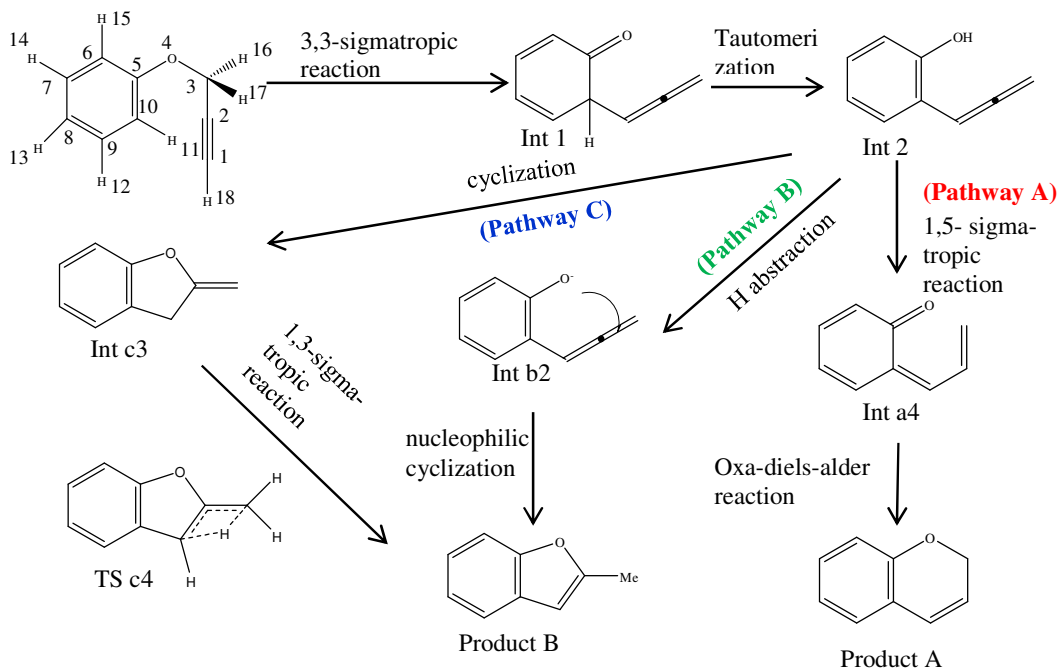
## References

- 1 A. M. M. Castro, *Chem. Rev.*, 2004, **104**, 2939.

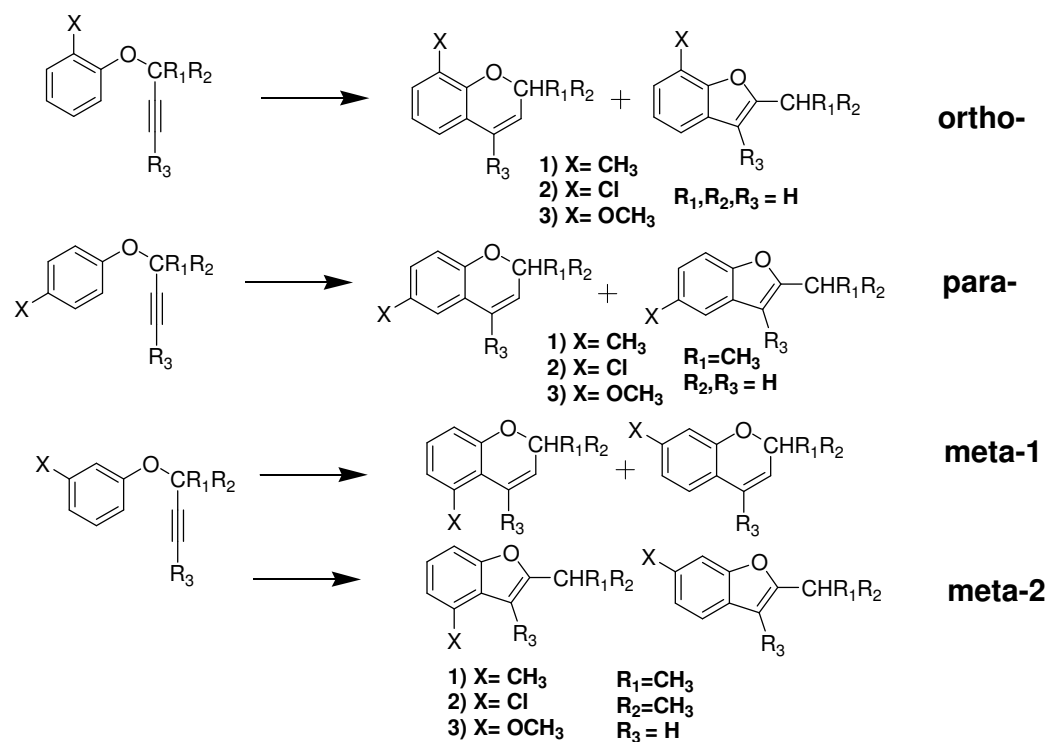
- 2 L. Claisen, *Chem. Ber.*, 1912, **45**, 3157.
- 3 I. Iwai and J. Ide, *Chem. Pharm. Bull.*, 1962, **10**, 926.
- 4 J. Zsindely and H. Schmidt, *Helv. Chim. Acta.*, 1968, **51**, 1510.
- 5 I. Iwai and J. Ide, *Chem. Pharm. Bull.*, 1963, **11**, 1042.
- 6 J. Hlubucek, E. Ritchie and W. C. Taylor, *Aust. J. Chem.*, 1971, **24**, 2347.
- 7 M. Harfenist and E. Thom, *J. Org. Chem.*, 1972, **37**, 841.
- 8 W. K. Anderson and E. J. Lavoie, *J. Org. Chem.*, 1973, **38**, 3832.
- 9 W. K. Anderson, E. J. Lavoie and P. G. Whitkop, *J. Org. Chem.*, 1974, **39**, 881.
- 10 H. Ishii, T. Ishikawa, S. Takeda, S. Ueki and M. Suzuki, *Chem. Pharm. Bull.*, 1992, **40**, 1148.
- 11 S. J. Pastine, S. W. Youn, and D. Sames, *Tetrahedron*, 2003, **59**, 8859
- 12 V. V. V. N. S. R. Rao, G. V. Reddy, R. Yadla, B. Narsaiah and P. S. Rao, *Arkivoc*, 2005, **iii**, 211.
- 13 S. A. Worlikar, T. Kesharwani, T. Yao and R. C. Larock, *J. Org. Chem.*, 2007, **72**, 1347.
- 14 R. S. Kenny, U. C. Mashelkar, D. M. Rane and D. K. Bezawada, *Tetrahedron*, 2006, **62**, 9280.
- 15 F. A. Khan and L. Soma, *Tetrahedron Lett.*, 2007, **48**, 85.
- 16 B. Lu, B. Wang, Y. Zhang and D. Ma, *J. Org. Chem.*, 2007, **72**, 5337.
- 17 A. K. Yadav, B. K. Singh, N. Singh and R. P. Tripathi, *Tetrahedron Lett.*, 2007, **48**, 6628.
- 18 N. R. Curtis, J. C. Prodger, G. Rassias and A. J. Walker, *Tetrahedron Lett.*, 2008, **49**, 6279.
- 19 V. S. P. R. Lingam, R. Vinodkumar, K. Mukkanti, A. Thomas and B. Gopala, *Tetrahedron Lett.*, 2008, **49**, 4260.
- 20 B. Godoi, A. Sperança, D. F. Back, R. Brandão, C. W. Nogueira and G. Zeni, *J. Org. Chem.*, 2009, **74**, 3469.
- 21 R. S. Menon, A. D. Findlay, A. C. Bissember and M. G. Banwell, *J. Org. Chem.*, 2009, **74**, 8901.
- 22 I. N. Lykakis, C. Efe, C. Gryparis and M. Stratakis, *Eur. J. Org. Chem.*, 2011, 2334.
- 23 C. L. Chung, C. H. Han, H. M. Wang, R. S. Hou and L. C. Chen, *J. Chin. Chem. Soc.*, 2001, **58**, 90.
- 24 N. Majumdar, K. A. Korthals, W. D. Wulff, *J. Am. Chem. Soc.*, 2012, **134**, 1357.
- 25 M. S. Dewar and E. F. Healy, *J. Am. Chem. Soc.*, 1984, **106**, 7127.
- 26 M. M. Khaledy, M. Y. S. Kalani, K. S. Khuong and K. N. Houk, *J. Org. Chem.*, 2003, **68**, 572.
- 27 S. Gül, F. Schoenebeck, V. Aviyente and K. N. Houk, *J. Org. Chem.*, 2010, **75**,

- 2115.
- 28 J. Rehbein, S. Leick and M. Hiersemann, *J. Org. Chem.*, 2009, **74**, 1531
- 29 O. Acevedo and K. Armacost, *J. Am. Chem. Soc.*, 2010, **132**, 1966.
- 30 Y. Zheng and J. Zhang, *J. Phys. Chem. A*, 2010, **114**, 4325.
- 31 A. D. Becke, *Phys. Rev. A*, 1988, **38**, 3098.
- 32 A. D. Becke, *J. Chem. Phys.* 1993, **98**, 5648.
- 33 A. D. Becke, *J. Chem. Phys.* 1997, **107**, 8554.
- 34 C. Lee, W. Yang and R. G. Parr, *Phys. Rev. B* 1988, **37**, 785.
- 35 H. L. Schmider,; A. D. Becke, *J. Chem. Phys.* 1998, **108**, 9624.
- 36 Y. Zhao and D. G. Truhlar, *Theor. Chem. Acc.*, 2008, **120**, 215.
- 37 Y. Zhao, N.E. Schultz, D.G. Truhlar, *J. Chem. Theory Comput.* 2006, **2**, 364.
- 38 J. P. Moreno, M. G. Kuzyk *J. Chem. Phys.* 2005, **123**, 194101.
- 39 J. D. Chai,; M. Head-Gordon, *Phys. Chem. Chem. Phys.* 2008, **10**, 6615.
- 40 A. D. Boese and J. M. L. Martin, *J. Chem. Phys.*, 2004, **121**, 3405.
- 41 S. Grimme, *J. Chem. Phys.*, 2006, **124**, 034108.
- 42 J. Tomasi, M. Persico, *Chem. Rev. (Washington, D.C.)*, 1994, **94**, 2027.
- 43 J. Tomasi, B. Mennucci, and R. Cammi, *Chem. Rev. (Washington, D.C.)* 2005, **105**, 2999.
- 44 Frisch, M. J.; Trucks, G. W.; Schlegel, H. B.; Scuseria, G. E.; Robb, M. A.; Cheeseman, J. R.; Scalmani, G.; Barone, V.; Mennucci, B.; Petersson, G. A.; et al. Gaussian 09, revision A.1; Gaussian, Inc.: Wallingford, CT, 2009.
- 45 E. D. Glendening, A. E. Reed, J. E. Carpenter and F. Weinhold, NBO 3.0 Program Manual
- 46 E. D. Glendening,; Landis, C. R., E. Weinhold, *WIREs Comput. Mol. Sci.* 2012, **2**, 1.
- 47 T. R. Ramadhar and R. A. Batey, *Computational and Theoretical Chemistry*, 2011, **976**, 167.
- 48 S. Yamabe, S. Okumoto, T. Hayashi, *J. Org. Chem.*, 1996, **61**, 6218.
- 49 J. Ho., M. L. Coote, *Theor. Chem. Acc.*, 2010, **125**, 3.
- 50 Liptak, M. D.; Gross, K. C.; Seybold, P. G.; Feldgus, S.; Shields, G. C. *J. Am. Chem. Soc.* **2002**, *124*, 6421.

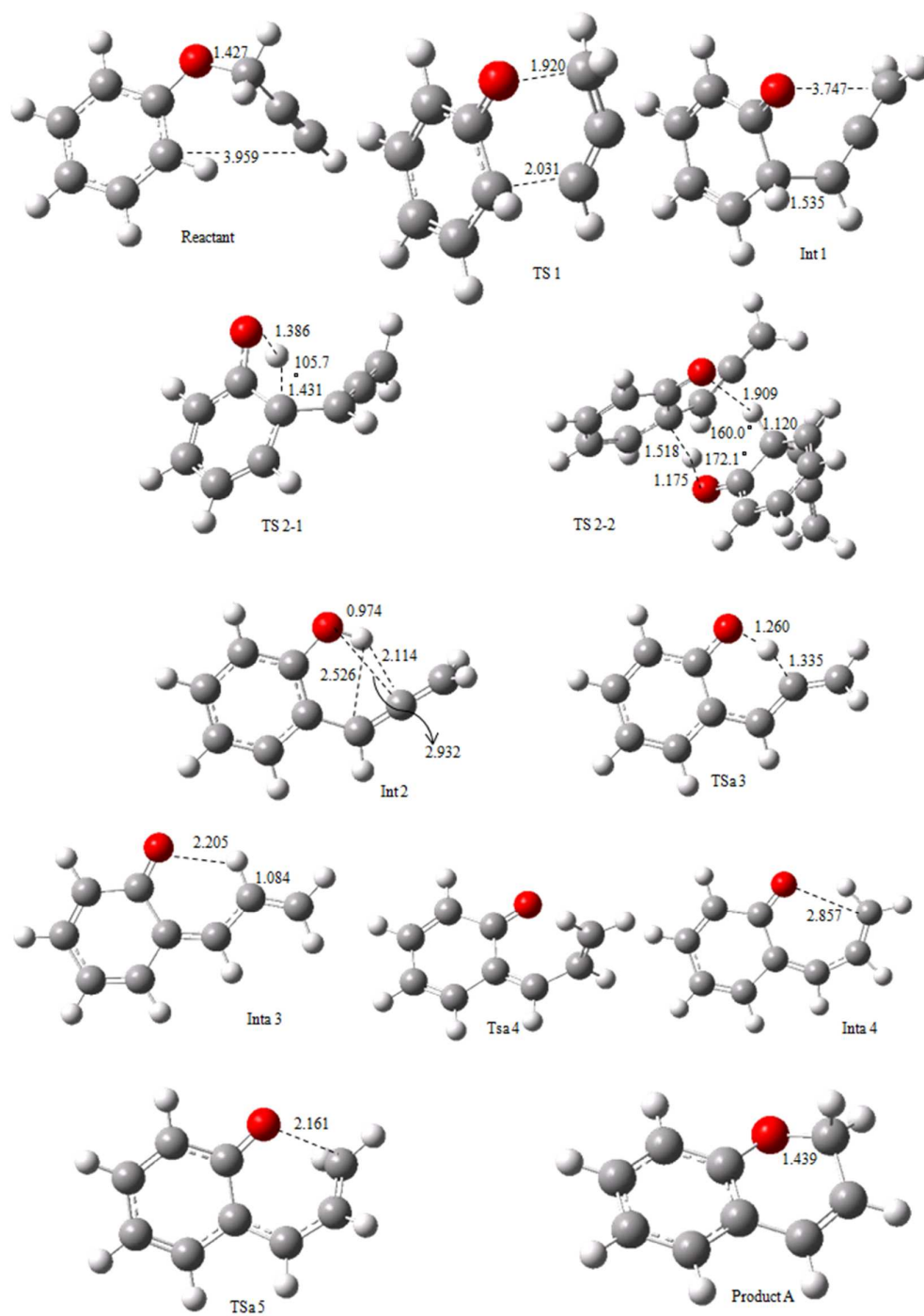
**Scheme 1:** The schematic representation of the mechanism for the formation of benzopyran and 2-Methylbenzofuran in aryl propargyl ether Claisen rearrangement.





**Scheme 2:** Various possible substitution at aryl and C3 position of alkyl group.

**Figure 1:** Optimized geometries at B3LYP/6-31+G\* level in gas phase (bond lengths in Å and bond angles in °)



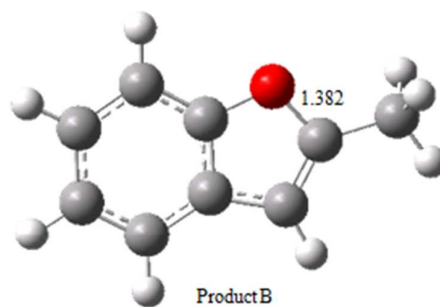
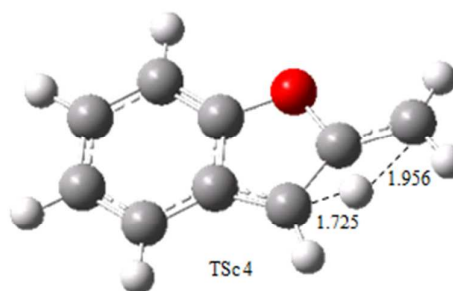
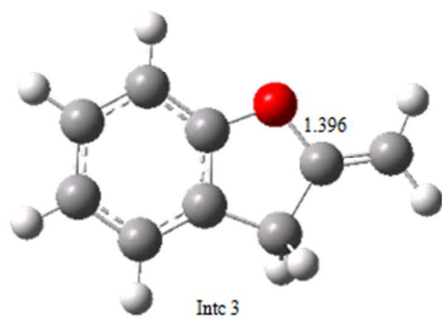
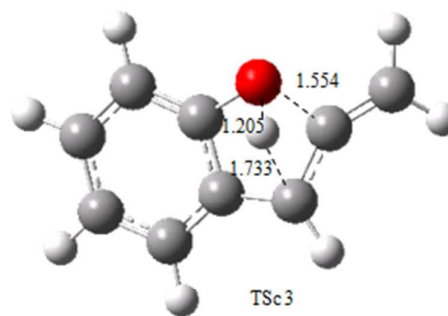
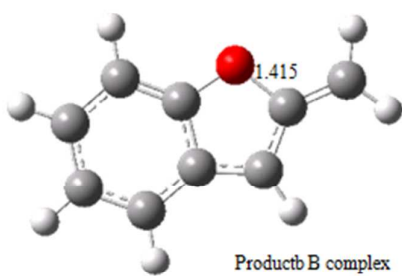
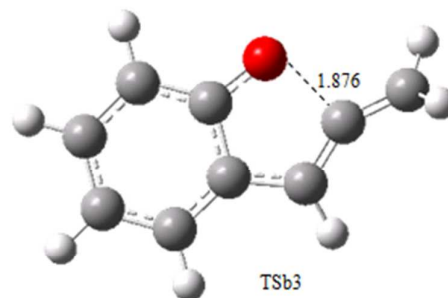
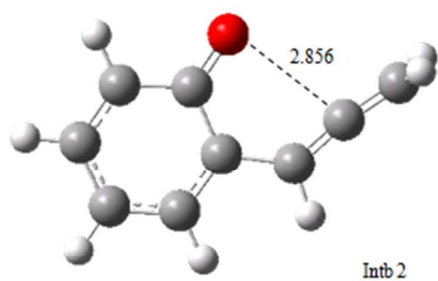


**Figure 2:** The computed Potential Energy Surface for aryl propargyl ether Claisen rearrangement in solvent phase at M06/6-31+G\*\*//B3LYP/6-31+G\* level of theory.

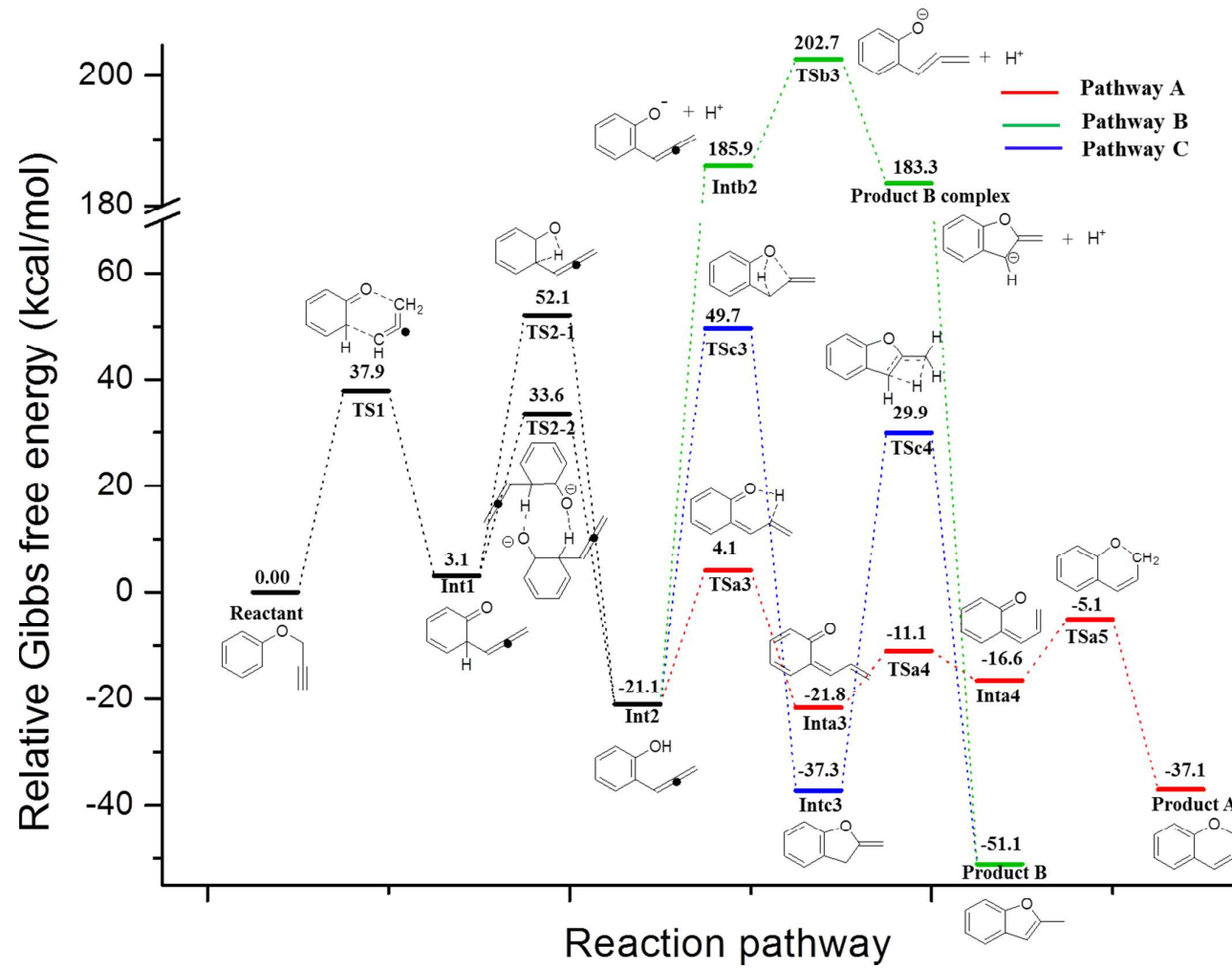


**Figure 3:** The geometries and the relative energies of reactant for different conformational isomerism in gas phase at M06/6-31+G\*\*// B3LYP/6-31+G\* level.

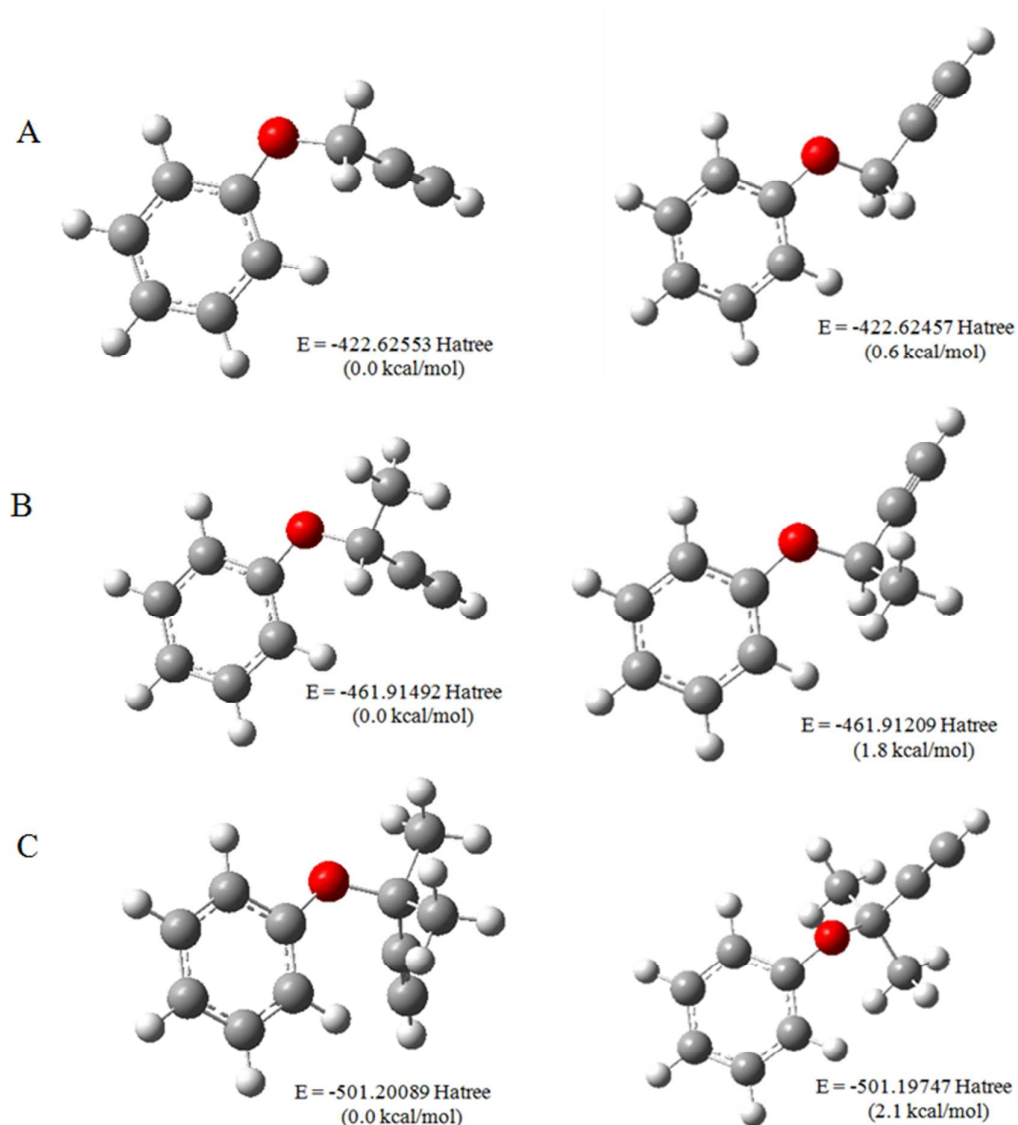


**Figure 4:** Three geometries of transition structures are chosen for NBO analysis to explore the substituent effect of the methyl group at C3-position. The bond distances are in Å°.

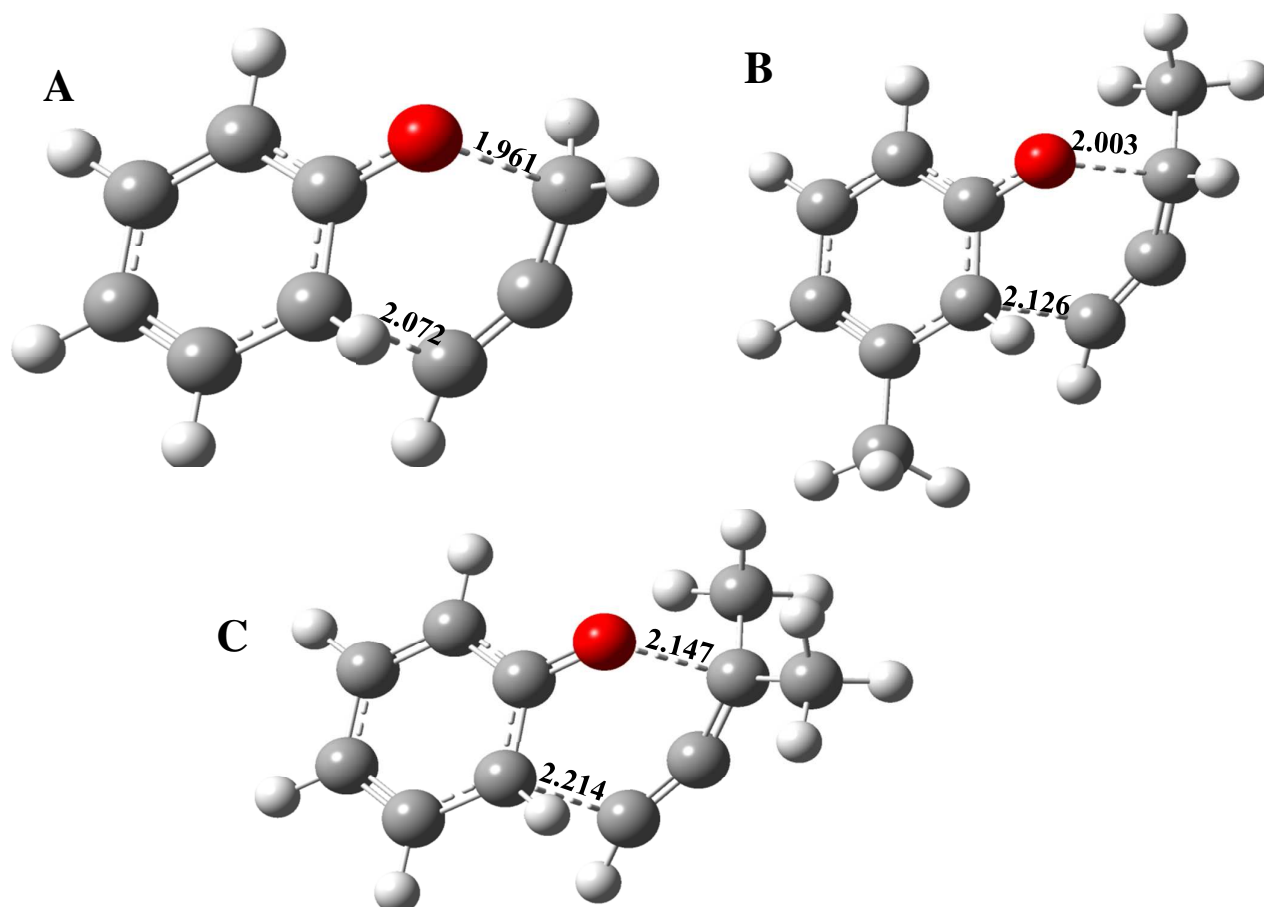


**Table 1:** Relative Gibbs free energy of the aryl propargyl ether Claisen Rearrangement at M06/6-31+G\*\*//B3LYP/6-31+G\* level (Unit: kcal/mol)

	M06/6-31+G **// B3LYP/6-31+G*	
	Gas	Solvent
Reactant	0.0	0.0
TS1	38.4	37.9
Int1	4.3	3.0
TS2-1	52.6	52.1
TS2-2	34.0	33.6
Int2	-20.5	-21.1
TSa3	5.1	4.1
Inta3	-20.2	-21.8
Tsa4	-10.0	-11.1
Inta4	-14.8	-16.6
TSa5	-3.9	-5.1
ProductA	-36.4	-37.1
Intb2	321.4	185.9
TSb3	336.1	202.7
Product B cpx	304.0	183.3
TSc3	49.9	49.7
Intc3	-37.3	-37.3
TSc4	30.6	29.9
ProductB	-51.3	-51.1

**Table 2:** Theoretical activation free energies of aryl propargyl ether Claisen rearrangement at B3LYP/6-31+G\* level optimization geometries and different DFT methods with the basis set 6-31+G\* for single point energy in N, N-diethylaniline. (Unit: kcal/mol)

	R1	R2	X	k×10 <sup>6</sup> , sec <sup>-1</sup> at 161.6 °C	ΔG <sup>‡</sup> (exp.) <sup>d</sup>	ΔG <sup>‡</sup> (calc.) <sup>e</sup>							
						B3LYP	M06-2X	M06	M05-2X	M05	wB97XD	BMK	B2PLYP
1	H	H	H	0.962	37.8	34.9	41.8	37.6	39.7	38.5	39.7	40.0	34.5
2	H	H	Cl	0.722	38.2	35.1	42.3	37.8	40.3	38.9	40.1	40.6	34.6
3	H	H	NO <sub>2</sub>	0.252	38.9	36.2	43.5	38.9	41.7	40.2	41.2	42.0	36.1
4	H	H	OCH <sub>3</sub>	1.15	37.6	34.8	42.8	37.8	40.8	38.8	40.3	40.8	34.4
5	CH <sub>3</sub>	H	H	3.49	36.6	33.4	41.0	35.5	39.3	37.1	38.5	39.8	33.4
6	CH <sub>3</sub>	H	Cl	3.79	36.5	33.6	41.5	35.8	39.9	37.3	38.9	40.0	33.7
7	CH <sub>3</sub>	H	NO <sub>2</sub>	2.27	37.0	33.9	42.2	35.9	40.7	37.5	39.4	40.6	34.6
8	CH <sub>3</sub>	H	OCH <sub>3</sub>	9.98	35.8	33.4	42.0	35.7	40.3	37.2	39.2	40.2	33.5
9	CH <sub>3</sub>	CH <sub>3</sub>	H	203	33.1	27.6	36.9	30.5	35.3	31.3	34.1	35.1	28.4
10	CH <sub>3</sub>	CH <sub>3</sub>	NO <sub>2</sub>	350	32.7	27.2	37.2	29.7	35.9	30.5	34.1	35.0	29.1
11	CH <sub>3</sub>	CH <sub>3</sub>	OCH <sub>3</sub>	628	32.2	27.5	38.0	30.8	36.7	31.0	35.1	35.3	28.6
R <sup>a</sup>						0.9861	0.9463	0.9825	0.9252	0.9847	0.9663	0.9627	0.9776
RMSE <sup>b</sup>						3.7	4.9	1.4	3.2	1.2	2.3	3.1	3.3
MUE <sup>c</sup>						3.5	4.8	1.0	3.1	1.1	2.2	3.0	3.2
Max. abs. error						5.5	6.2	3.0	4.5	2.2	3.4	4.4	4.7

R<sup>a</sup> = Pearson correlation coefficient; RMSE<sup>b</sup> = root-mean-square error; MUE<sup>c</sup> = Mean Unsigned Error; exp.<sup>d</sup>: experimental values; calc.<sup>e</sup> = calculated



**Table 3:** Theoretical activation free energies of aryl propargyl ether Claisen rearrangement at B3LYP/6-31+G\* level optimization geometries and M06 single point energy calculation with different basis sets in N, N-diethylaniline. (Unit: kcal/mol)

	R1	R2	X	$k \times 10^6, \text{sec}^{-1}$ at 161.6 °C	$\Delta G^\ddagger(\text{exp.})^d$	M06					
						$\Delta G^\ddagger(\text{calc.})^e$					
						6-31+G*	6-31+G**	6-31++G*	6-311++G**	6-311++G(2d,p)	6-311++G(2d,2p)
1	H	H	H	0.962	37.8	37.6	37.6	37.5	38.9	38.9	38.9
2	H	H	Cl	0.722	38.2	37.8	37.8	37.8	38.9	39.0	39.1
3	H	H	NO <sub>2</sub>	0.252	38.9	38.9	38.9	38.8	39.7	39.9	40.0
4	H	H	OCH <sub>3</sub>	1.15	37.6	37.8	37.8	37.7	38.8	38.9	39.0
5	CH <sub>3</sub>	H	H	3.49	36.6	35.5	35.6	35.4	36.4	36.7	36.8
6	CH <sub>3</sub>	H	Cl	3.79	36.5	35.8	35.8	35.7	36.6	36.9	37.0
7	CH <sub>3</sub>	H	NO <sub>2</sub>	2.27	37.0	35.9	36.0	35.9	36.5	37.0	37.1
8	CH <sub>3</sub>	H	OCH <sub>3</sub>	9.98	35.8	35.7	35.8	35.7	36.6	36.9	37.0
9	CH <sub>3</sub>	CH <sub>3</sub>	H	203	33.1	30.6	30.7	30.7	31.1	31.5	31.6
10	CH <sub>3</sub>	CH <sub>3</sub>	NO <sub>2</sub>	350	32.7	29.7	29.9	29.6	30.2	30.7	30.8
11	CH <sub>3</sub>	CH <sub>3</sub>	OCH <sub>3</sub>	628	32.2	34.8	33.3	34.9	34.8	34.7	35.1
$R^a$						0.8662	0.9330	0.8585	0.8977	0.9161	0.9041
RMSE <sup>b</sup>						1.5	1.3	1.5	1.4	1.3	1.4
MUE <sup>c</sup>						1.1	0.9	1.1	1.1	1.1	1.2
Max. abs. error						3.0	2.8	3.1	2.6	2.5	2.9

$R^a$  = Pearson correlation coefficient;  $\overline{\text{RMSE}}^b$  = root-mean-square error;  $\overline{\text{MUE}}^c$  = Mean Unsigned Error; exp.<sup>d</sup>: experimental values; calc.<sup>e</sup> = calculated

**Table 4:** The energy barrier of the first two steps of methyl group on aromatic segment with zero, mono **and** dimethyl groups on the aliphatic segment in N, N-diethylaniline at M06/6-31+G\*\*//B3LYP/6-31+G\* level.

	Parent	1a-o	1a-p	1a-m1	1a-m2	1b-o	1b-p	1b-m1	1b-m2	1c-o	1c-p	1c-m1	1c-m2
Step1	37.9	37.0	38.2	37.7	36.7	35.3	36.7	36.1	35.5	29.9	31.4	31.9	30.3
Step2	30.6	30.1	30.9	28.4	29.4	31.3	33.2	30.9	31.7	31.2	33.8	31.1	30.0

\* ortho- is denoted by o-; para- is denoted by p-; meta-1 is denoted by m1; meta-2 is denoted by m2.; a,b and c represents the zero, mono **and** dimethyl group on the aliphatic segment, respectively.

**Table 5:** The energy barrier of the first two steps of chloro group on aromatic segment with zero, mono **and** dimethyl groups on the aliphatic segment in N, N-diethylaniline at M06/6-31+G\*\*//B3LYP/6-31+G\* level.

	Parent	2a-o	2a-p	2a-m1	2a-m2	2b-o	2b-p	2b-m1	2b-m2	2c-o	2c-p	2c-m1	2c-m2
Step1	37.9	36.4	38.1	37.7	36.7	34.2	36.0	35.8	34.8	29.0	30.6	30.2	29.4
Step2	30.6	30.3	31.5	29.7	31.1	31.5	32.9	30.3	32.1	31.9	33.7	30.1	32.9

\* ortho- is denoted by o-; para- is denoted by p-; meta-1 is denoted by m1; meta-2 is denoted by m2.; a,b and c represents the zero, mono **and** dimethyl group on the aliphatic segment, respectively.

**Table 6:** The energy barrier of the first two steps of methoxy group on aromatic segment with zero, mono **and** dimethyl groups on the aliphatic segment in N, N-diethylaniline at M06/6-31+G\*\*//B3LYP/6-31+G\* level.

	Parent	3a-o	3a-p	3a-m1	3a-m2	3b-o	3b-p	3b-m1	3b-m2	3c-o	3c-p	3c-m1	3c-m2
Step1	37.9	36.1	38.0	35.3	33.6	34.2	36.0	35.6	33.9	29.3	31.0	31.0	29.2
Step2	30.6	31.8	32.5	27.7	25.9	32.0	34.3	26.4	28.3	32.0	35.5	25.4	27.8

\* ortho- is denoted by o-; para- is denoted by p-; meta-1 is denoted by m1; meta-2 is denoted by m2.; a,b and c represents the zero, mono **and** dimethyl group on the aliphatic segment, respectively.

**Table 7:** Selected donor-acceptor bond orbital interaction and  $\Delta E_2$  values (kcal/mol) for transition state species (geometries in Figure 4) of aryl propargyl ether Claisen rearrangement.<sup>a</sup>

species	donor	acceptor	interaction	E(2)
A	BD C1-C10	BD* C5-O4	$\sigma \rightarrow \pi^*$	27.25
	BD C1-C10	BD* C2-C3	$\sigma \rightarrow \pi^*$	18.8
	BD C5-O4	BD* C2-C3	$\pi \rightarrow \pi^*$	25.33
	BD* C5-O4	BD* C2-C3	$\pi^* \rightarrow \pi^*$	85.7
B	BD C1-C10	BD* C5-O4	$\sigma \rightarrow \pi^*$	30.89
	BD C1-C10	BD* C2-C3	$\sigma \rightarrow \pi^*$	20.93
	BD C5-O4	BD* C2-C3	$\pi \rightarrow \pi^*$	15.08
	BD* C5-O4	BD* C2-C3	$\pi^* \rightarrow \pi^*$	74.29
C	BD C1-C10	BD* C5-O4	$\sigma \rightarrow \pi^*$	33.24
	BD C1-C10	BD* C2-C3	$\sigma \rightarrow \pi^*$	22.16
	BD C5-O4	BD* C2-C3	$\pi \rightarrow \pi^*$	9.99
	BD* C5-O4	BD* C2-C3	$\pi^* \rightarrow \pi^*$	61.32

<sup>a</sup> NBO analysis is performed at the M06/6-31+G\*\*// B3LYP/6-31+G\* level. BD and BD\* denote the occupied bond and formally empty antibonding orbital, respectively.